Journal of Enzyme Inhibition and Medicinal Chemistry

ISSN: 1475-6366 (Print) 1475-6374 (Online) Journal homepage: informahealthcare.com/journals/ienz20

Effect of tetrahydropteridines on the monophenolase and diphenolase activities of tyrosinase

F. García Molina, J. L. Muñoz, R. Varón, J. N. Rodríguez López, F. García Cánovas & J. Tudela

To cite this article: F. García Molina, J. L. Muñoz, R. Varón, J. N. Rodríguez López, F. García Cánovas & J. Tudela (2007) Effect of tetrahydropteridines on the monophenolase and diphenolase activities of tyrosinase, Journal of Enzyme Inhibition and Medicinal Chemistry, 22:4, 383-394, DOI: 10.1080/14756360701189776

To link to this article: https://doi.org/10.1080/14756360701189776

Journal of Enzyme Inhibition and Medicinal Chemistry, August 2007; 22(4): 383–394

informa
healthcare

Effect of tetrahydropteridines on the monophenolase and diphenolase activities of tyrosinase

F. GARCÍA MOLINA[1], J. L. MUÑOZ[1], R. VARÓN[2], J. N. RODRÍGUEZ LÓPEZ[1], F. GARCÍA CÁNOVAS[1], & J. TUDELA[1]

[1]*GENZ: Grupo de Investigación de Enzimología, Departamento de Bioquímica y Biología Molecular-A, Facultad de Biología, Universidad de Murcia, E-30100 Espinardo, Murcia, Spain, and* [2]*Departamento de Química-Física. Escuela Politécnica Superior, Universidad de Castilla la Mancha. Avda. España s/n. Campus Universitario, E-02071, Albacete, Spain*

(Received 20 July 2006; in final form 30 November 2006)

Abstract

This study explains the action of compounds such as 6-tetrahydrobiopterin, ($6BH_4$) and 6,7-dimethyltetrahydrobiopterin (6,7-di-CH_3BH_4) on the monophenolase and diphenolase activities of tyrosinase. These reductants basically act by reducing the *o*-quinones, the reaction products, to *o*-diphenol. In the case of the diphenolase activity a lag period is observed until the reductant is depleted; then the system reaches the steady-state. In the action of the enzyme on monophenol substrates, when the reductant concentration is less than that of the *o*-diphenol necessary for the steady-state to be reached, the system undergoes an apparent activation since, in this way, the necessary concentration of *o*-diphenol will be reached more rapidly. However, when the reductant concentration is greater than that of the *o*-diphenol necessary for the steady-state to be reached, the lag period lengthens and is followed by a burst, by means of which the excess *o*-diphenol is consumed, the steady-state thus taking longer to be reached. Moreover, in the present kinetic study, we show that tyrosinase is not inhibited by an excess of monophenol, although, to confirm this, the system must be allowed to pass from the transition state and enter the steady-state, which is attained when a given amount of *o*-diphenol has accumulated in the medium.

Keywords: *Activation, inhibition, monophenol,* o-*diphenol, melanogenesis, coenzymes, tyrosinase*

Introduction

In their catalytic action on substrates, most enzymes rapidly reach the steady-state after a transition phase lasting in the order of milliseconds. However, there is a wide-ranging group of enzymes, the so-called hysteretic enzymes, that show a slow response (seconds-minutes scale) when substrate is added. The origin of this slow response is diverse, but may include isomerisation, polymerisation or dissociation processes, etc. [1].

Tyrosinase catalyses the hydroxylation of monophenols (M) to *o*-diphenols (D) and their subsequent oxidation to *o*-quinone (Q), in both cases using molecular oxygen [2,3].

Tyrosinase might be included in the group of hysteretic enzymes, although its slow response with monophenols has a different kinetic basis: the accumulation of L-dopa in the reaction medium from the *o*-dopaquinone generated by the action of tyrosinase on L-tyrosine, until the system finally reaches the steady-state. The kinetic behaviour of tyrosinase is very complex due to the simultaneous occurrence of the enzymatic oxidation of monophenol and *o*-diphenol to *o*-quinone, on the one hand, and the coupled non-enzymatic reactions of *o*-quinone, on the other [4].

Recently a series of publications has been published on the regulation of tyrosinase by tetrahydropteridines, (6-R)-L-erythro-5,6,7,8-tetrahydro biopterin

Correspondence: F. García Canovas, GENZ: Grupo de Investigación de Enzimología, Departamento de Bioquímica y Biología Molecular-A, Facultad de Biología, Universidad de Murcia, E-30100 Espinardo, Murcia, Spain. Fax: 34 968 364147. E-mail: canovasf@um.es, http://www.um.es/genz

ISSN 1475-6366 print/ISSN 1475-6374 online
DOI: 10.1080/14756360701189776

($6BH_4$) [5–9]. As regards this regulation, particularly the enzyme's inhibition by $6BH_4$, it has been suggested that this cofactor acts as a non-competitive inhibitor [5]. Prior to studying the action of $6BH_4$ on tyrosinase, the authors, quite logically, studied the enzyme's action kinetic on L-tyrosine [5,7] and noted in all cases an inhibition caused by an excess of substrate, depicted as $1/V_{ss}^{M,DC}$ *vs* $1/[M]_0$, where $V_{ss}^{M,DC}$ indicates the apparent steady-state rate of tyrosinase acting on L-tyrosine (measured from the formation of dopachrome), and $[M]_0$ is the initial concentration of monophenol. However, according to our model such inhibition through an excess of monophenol does not occur, despite the fact that it has been described by several authors [5,7,10–12] probably because of the difficulties involved in accurately measuring the rate during the steady-state. It is therefore necessary to wait until the system reaches the steady-state because, if this is not reached, apparent inhibitions by substrate and reductants, such as $6BH_4$ and by 6,7-(R,S)-dimethyl tetrahydropterine (6,7-di-CH_3BH_4), and also with ascorbic acid (AH_2), may appear.

In this paper, we describe the action of tyrosinase on monophenol and *o*-diphenol, and demonstrate that the enzyme does not undergo inhibition by excess of monophenol. The proposed mechanism, Scheme I, also explains the action of reductants such as 6-BH_4, 6,7-di-CH_3BH_4 and AH_2.

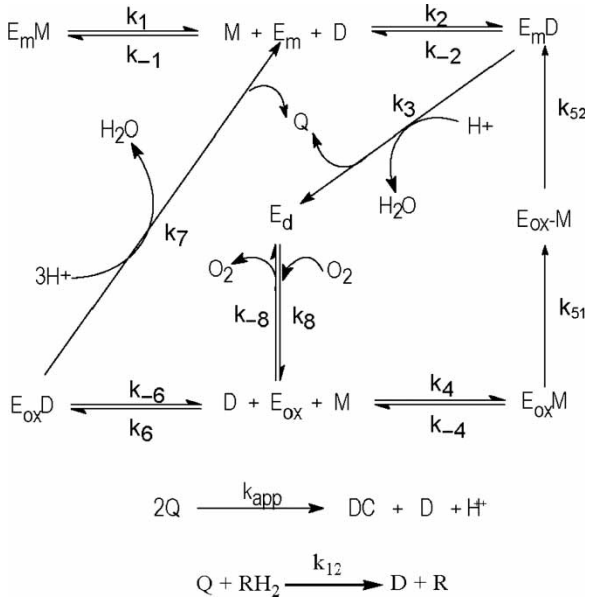

Scheme I. Suggested kinetic reaction mechanism of tyrosinase acting on monophenol and *o*-diphenol, with the non-enzymatic reactions corresponding to the evolution of *o*-quinone (Ros et al., 1994 [18]). Where M is monophenol, D is *o*-diphenol, E is enzyme tyrosinase, E_d is *Desoxy*tyrosinase, E_m is *Met*tyrosinase, E_mM is *Met*tyrosinase monophenol binding complex, E_mD is *Met*tyrosinase *o*-diphenol binding complex, E_{ox} is *Oxy*tyrosinase, $E_{ox}M$ is *Oxy*tyrosinase monophenol binding complex, E_{ox}-M is covalently bound *oxy*tyrosinase monophenol, $E_{ox}D$ is covalently bound *oxy*tyrosinase *o*-diphenol, Q is *o*-quinone, DC is dopachrome, and RH_2 is reductant.

Materials and methods

Reagents

L-Tyrosine, L-dopa, (6-R)-L-erythro-5,6,7,8-tetrahydro-biopterin dihydrochloride ($6BH_4$), 6,7-(R,S)-dimethyl 5,6,7,8-tetrahydropterin monohydrochloride (6,7-di-CH_3BH_4) and ascorbic acid (AH_2) were purchased from Sigma (Madrid, Spain). Stock solutions of the phenolic substrate were prepared in 0.15 mM phosphoric acid to prevent autoxidation. $6BH_4$ and 6,7-di-CH_3BH_4 were prepared in 0.15 mM phosphoric acid, eliminating the oxygen by passing a current of nitrogen. The AH_2 was prepared in previously de-aired water to prevent autoxidation. The monophenol was purified according to [11].

Enzyme source

Mushroom tyrosinase (3000 U/mg) was purchased from Sigma (Madrid, Spain) and purified according to [13]. The enzyme concentration was calculated taking the value of M_r as 120,000. Protein content was determined by Bradford's method [14] using bovine serum albumin as standard.

Spectrophotometric assays

Absorption spectra with a 60 nm/s scanning speed were recorded in an ultraviolet-visible Perkin-Elmer Lambda-2 spectrophotometer, online interfaced with a compatible PC 486DX microcomputer and controlled with the Perkin-Elmer UVWINLAB software. Temperature was controlled at 25°C using a Haake D1G circulating water-bath with a heater/cooler and checked using a Cole-Parmer digital thermometer with a precision of ± 0.1°C. Kinetic assays were also carried out with the above instruments by measuring the appearance of the products in the reaction medium. Reference cuvettes contained all the components except the substrate, with a final volume of 1 ml. All the assays were carried out under conditions of tyrosinase saturation by molecular oxygen (0.26 mM in the assay medium) [15]. The reactions were followed at a wavelength $\lambda = 475$ nm, (dopachrome maximum), and $\varepsilon = 3600\ M^{-1}\ cm^{-1}$.

Simulation assays

The numerical integration is based on the Runge-Kutta-Fehlberg algorithm [16], implemented on a PC-compatible computer program (WES) [17].

Results

As stated above, the object of this work was to show that tyrosinase is not inhibited by an excess of

monophenol or by reductants such as $6BH_4$, 6,7 di-CH_3BH_4 and AH_2, when the experimental measurements are made in the true steady-state. For this purpose, we carried out a series of experiments to ensure that enzyme activity was being measured accurately.

In the case of any enzymatic system, including tyrosinase, the steady-state rate should be linear with respect to enzyme concentration, and so, two types of experiment must be carried out to determine the following:

(a) The steady-state rate of the enzyme acting on substrate (V_{ss}) at different initial concentrations of enzyme, while other variables, such as substrate concentration [S], pH, temperature and ionic strength are kept constant. The kinetic analysis shows that V_{ss} will be linear with respect to $[E]_0$ for the mechanism of Scheme IS, (Supplementary material, Figure S1).

(b) The steady-state rate V_{ss} at different initial concentrations of substrate, while keeping the other variables constant, $[E]_0$, pH, temperature and ionic strength, constant. The kinetic analysis in this case predicts a hyperbolic relation for the mechanism of Scheme IS, V_{ss} *vs* $[S]_0$, (Supplementary material, Figure 1S) or a non-hyperbolic dependence for the mechanism of Scheme IIS (Supplementary material, Figure 1S Inset), although the linearity of V_{ss} *vs* $[E]_0$ will be maintained (Supplementary material, Figure 1S and Figure 1S Inset).

In the case of the tyrosinase enzymatic system, when the enzyme acts on monophenols, the test which indicates that the steady-state rates are correct is that which shows that the steady-state rate is linear with respect to enzyme concentration (i.e.: $V_{ss}^{M,DC}$ *vs* $[E]_0$ must be a straight line).

Since tyrosinase shows a lag period when it acts on monophenols, care should be taken to ensure that the steady-state measurements really correspond to the steady-state of the system; only in this way will any conclusions concerning the action of inhibitors/activators be valid. To ensure this, the following experiments were carried out.

Effect of initial monophenol and enzyme concentrations on tyrosinase activity

When the enzyme begins to act on monophenol, (see Scheme I) dopachrome (DC) originates from the *o*-quinone formed and *o*-diphenol is regenerated in the reaction medium, so that the enzyme needs time to reach the steady-state; this is the lag period (τ) that is characteristic of monophenolase activity. As has been demonstrated experimentally [4] and by simulating the reactions evolving according to the mechanism of Scheme l [18], the length of the lag period diminishes as $[E]_0$ increases and $[M]_0$ is kept constant, while it lengthens when $[M]_0$ is increased and $[E]_0$ is kept constant. This is reflected in the results of the experiments depicted in Figure 1.

In Figure 1, curve (a) shows the lag period (τ_1), which is calculated when the system reaches the steady-state with a velocity of $V_1^{M,DC}$. When $[M]_0$ is increased and $[E]_0$ is kept constant, the system takes more time to reach the steady-state (curve b) after a lag period (τ_2), with ($\tau_2 > \tau_1$) and $V_2^{M,DC} > V_1^{M,DC}$. The effect of increasing $[E]_0$ while $[M]_0$ remains constant is shown in the same figure; in this case, the system takes less time to reach the steady-state (curve c), while $V_3^{M,DC} > V_1^{M,DC}$. Similar results were obtained in a simulation of the mechanism of Scheme I (Supplementary material, Figure S2).

Variation in the initial concentration of enzyme

Figure 2 shows the rates measured in the tyrosinase action on monophenol when the enzyme concentration is varied. Note that if the measurements are made on the same time scale, determining the increase in absorbance at a fixed time after the beginning of the reaction, the apparent values of $V_{ss}^{M,DC}$ obtained are not linear with $[E]_0$ (curve a). However, if the measurements of $V_{ss}^{M,DC}$ are made on different time scales and ensuring that the system has reached the steady-state, $V_{ss}^{M,DC}$ is linear with $[E]_0$ (curve b). It should be emphasised that even if the substrate has caused inhibition, V_{ss} *vs* $[E]_0$ will still be linear. (see Figure S1 Inset). Figure 2 also shows how the lag period

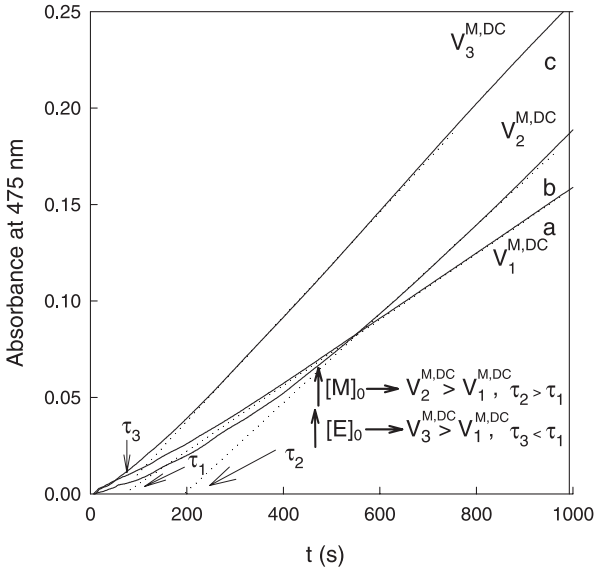

Figure 1. Spectrophotometric register of dopachrome accumulation versus action time of tyrosinase on L-tyrosine. Curve (a): $[M]_0 = 0.36$ mM and $[E]_0 = 7$ nM. Curve (b): same enzyme concentration as (a) and $[M]_0 = 1$ mM. Curve (c): same substrate concentration as (a) and $[E]_0 = 14$ nM.

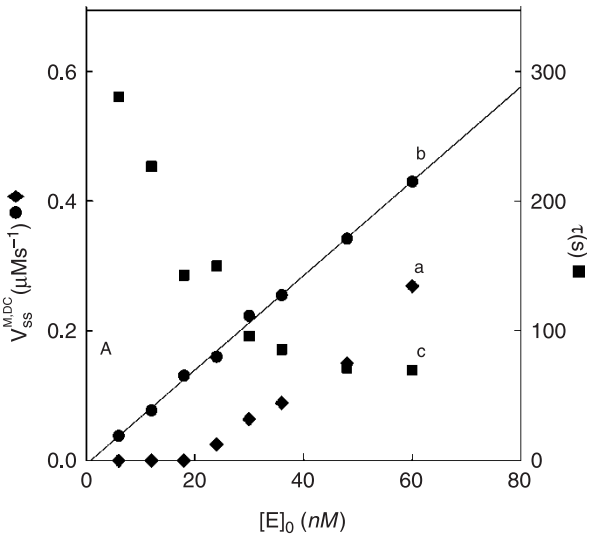

Figure 2. Representation of the values of rate of tyrosinase acting on L-tyrosine ($V_{ss}^{M,DC}$), and of the lag period with respect to enzyme concentration. [M]$_0$ = 0.25 mM. • Values of $V_{ss}^{M,DC}$ obtained in the true steady-state. ◆ Rate values obtained considering the increase in absorbance at a fixed time from beginning of reaction. ■ Values of lag period.

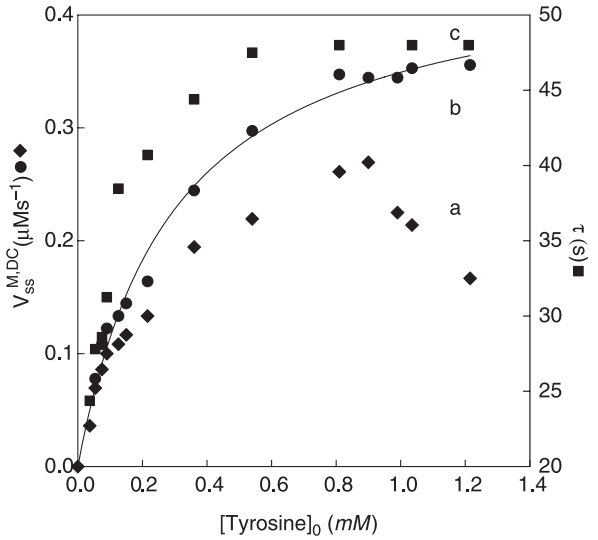

Figure 3. Representation of the rate of tyrosinase acting on L-tyrosine ($V_{ss}^{M,DC}$), and of the lag period (τ) with different substrate concentrations. [E]$_0$ = 45 nM, • Values of $V_{ss}^{M,DC}$ obtained in the true steady-state. ▲ Rate values obtained considering the increase in absorbance at a fixed time from beginning of reaction, three min. ■ Values of lag period.

decreases as the enzyme concentration increases. Similar results were obtained by simulation of Scheme I (Supplementary material, Figure S3).

Variation in substrate concentration

The experiment depicted in Figure 3 shows the $V_{ss}^{M,DC}$*vs* [M]$_0$ when the enzyme concentration is kept constant. If $V_{ss}^{M,DC}$ is measured from the increase in absorbance at a fixed time from the beginning of the experiment, curve (a) of Figure 3 is obtained. However, if the system is allowed to reach the steady-state, the representation of $V_{ss}^{M,DC}$ *vs* [M]$_0$ is an hyperbola (curve b) for L-tyrosine, (V_{max} = (0.36 ± 0.03) μMs^{-1}; K_m = (0.20 ± 0.06) mM). Note that the lag period, τ, increases with the increasing concentration of substrate (curve c). Similar results were obtained by simulation of Scheme I (Supplementary material, Figure S4).

In addition, the kinetic analysis of the mechanism of Scheme 1 provides an analytical expression for $V_{ss}^{M,DC}$of the type [18]:

$$V_{ss}^{M,DC} = \frac{V_{\max}^{M,DC}[\mathrm{M}]_0[\mathrm{O_2}]_0}{K_m^M K_s^{O_2} + K_M^{O_2(M)}[\mathrm{M}]_0 + K_m^M[\mathrm{O_2}]_0 + [\mathrm{M}]_0[\mathrm{O_2}]_0} \quad (1)$$

where

$$V_{\max}^{M,DC} = k_{cat}^M[\mathrm{E}]_0 = \frac{k_{51}k_{52}}{k_{51}+k_{52}}[\mathrm{E}]_0 \quad (2)$$

$$K_m^M = \frac{k_{cat}^M}{k_4} \quad (3)$$

$$K_m^{O_2(M)} = \frac{3k_{cat}^M}{2k_8} \quad (4)$$

$$K_s^{O_2} = \frac{k_{-8}}{k_8} \quad (5)$$

Equations (2–5) show $V_{\max}^{M,Cr}$, the maximum dopachrome accumulation rate (Equation (2)); k_{cat}^M, the catalytic constant of the enzyme acting on monophenols (Equation (2)); K_m^M, the Michaelis-Menten constant for monophenol (Equation (3)); $K_m^{O_2(M)}$, the Michaelis-Menten constant for the oxygen in the presence of monophenol (Equation (4)); $K_s^{O_2}$, the dissociation constant of oxygen from the form E_{ox} (Equation (5)). Since the [O$_2$]$_0$ is saturating [4] Equation (1) can be simplified to:

$$V_{ss}^{M,DC} = \frac{V_{\max}^{M,DC}[\mathrm{M}]_0}{K_m^M + [\mathrm{M}]_0} \quad (6)$$

which fulfils the tests described in Figure S1. Note the linear dependence of $V_{ss}^{M,DC}$ *vs* [E]$_0$ and the hyperbolic dependence of $V_{ss}^{M,DC}$ *vs* [M]$_0$.

Action of 6BH$_4$ on monophenolase activity

Figure 4 depicts the activity of tyrosinase on L-tyrosine at different concentrations of 6BH$_4$ and 6,7-di-CH$_3$BH$_4$. When the rate is measured as an

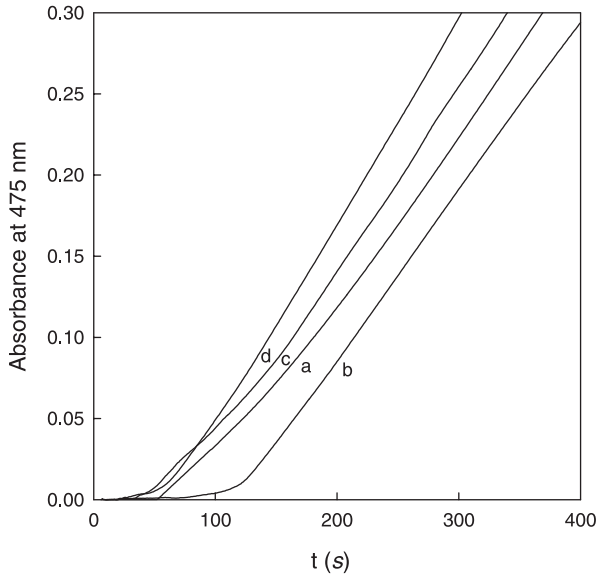

Figure 4. Action of reductants on monophenolase activity of tyrosinase. Effect of $6BH_4$ and 6,7-di-CH_3BH_4. Effect of $6BH_4$. $[L\text{-tyrosine}]_0 = 0.9$ mM, $[E]_0 = 30$ nM. The concentrations of $6BH_4$ were (a) 0; (b) 80 μM; (c) 10 μM and (d) 25 μM.

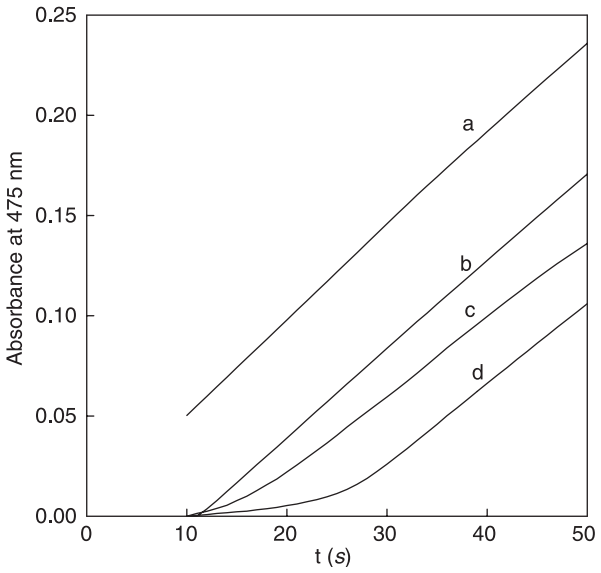

Figure 5. Effect of reductants on the diphenolase activity of tyrosinase. Effect of $6BH_4$. Spectrophotometric registers of the accumulation of dopachrome in the action of tyrosinase on L-dopa. The experimental conditions were: The initial concentration of *o*-diphenol $[D]_0 = 1$ mM, $[E]_0 = 15$ nM. The values of $[6BH_4]_0$ were: (a) 0; (b) 10 μM; (c) 20 μM and (d) 60 μM.

increase of absorbance at a fixed time, apparent activations are obtained at low concentrations of $6BH_4$, (curves c and d) while at high concentrations of $6BH_4$ there is an apparent inhibition (curve b). Note that the lines are parallel at long times, that is, the rates are equal when the system has reached the steady-state. Similar results were obtained by simulation of the mechanism of Scheme I (Supplementary material, Figure S5).

Action of $6BH_4$ on diphenolase activity

Figure 5 shows the effect of $6BH_4$ on the diphenolase activity of tyrosinase. The curve (a) of Figure 5 corresponds to the reaction of L-dopa with tyrosinase; as can be seen, the system rapidly reaches the steady-state and the lag period cannot be measured. In (b), (c) and (d), the concentration of $6BH_4$ gradually increases, giving rise to a lag period due to the reduction of *o*-quinone by means of $Q + RH_2 \xrightarrow{k_{12}} D + R$ (Scheme I), where RH_2 indicates the presence of a reductant. Note that, once $6BH_4$ has been consumed, the straight lines are parallel, data that are in agreement with those of other authors [6]. Similar results are obtained using AH_2 as reductant (data not shown). Similar results were obtained by simulation of the mechanism of Scheme I (Supplementary material, Figure S6).

Effect of $6BH_4$ on the steady-state of monophenolase activity

Figure 6 depicts an experiment involving monophenolase activity to which a given quantity of *o*-diphenol is added at t = 0. In this case, the system shows no lag period, curve (a). The addition of increasing quantities of $6BH_4$ increases the lag phase before proceeding to the steady-state, as shown by the

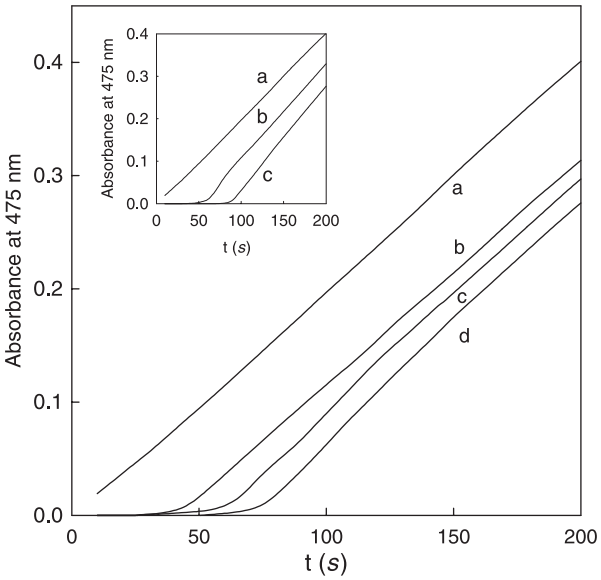

Figure 6. Effect of reductants on the monophenolase activity of tyrosinase in the steady-state. The steady-state was reached rapidly adding a quantity of *o*-diphenol so that $[D] = [D]_{ss} = R[M]_0$ with $R = (V^{M,DC}_{max} K^D_m)/(2V^{D,DC}_{max} K^M_m)$. $[M]_0 = 0.9$ mM, $[E]_0 = 62$ nM, $[D]_{ss} = 45$ μM. Effect of $6BH_4$. The concentrations of $6BH_4$ were: a) 0; (b) 50 μM; (c) 65 μM and (d) 75 μM, respectively. Inset: Effect of AH_2. The values of initial concentration of ascorbic acid $[AH_2]_0$ were (a) 0; (b) 50 μM and (c) 75 μM.

parallel lines. Similar results were obtained in a simulation of the mechanism of Scheme I (Supplementary material, Figure S7).

Discussion

Effect of initial monophenol and enzyme concentrations on tyrosinase activity

From the experiments depicted in Figure 1, it can be concluded, that the lag period (τ) diminishes with increasing $[E]_0$ and increases with increasing $[M]_0$, which implies that $V_{ss}^{M,DC}$ cannot be determined experimentally on the same time scale, as would be the case with a Michaelian enzyme not showing a lag period. In the experiments described below, we shall see how measurements made on the same time scale lead to error.

The experiments depicted in Figure 2 confirm the validity of the mechanism (Scheme I) and the need to make measurements on different time scales when $[E]_0$ or $[M]_0$ varies.

Equation (6) differs from that proposed by other authors (Equation (7)) [5] to explain the action of tyrosinase on monophenols

$$V_{ss}^{M,DC} = \frac{V_{\max}^{M,DC}[M]_0}{K_m^M + [M]_0\left(1 + \frac{[M]_0}{K_{si}}\right)} \qquad (7)$$

where K_{si} is the substrate inhibitor constant. Note the differences between Equations (6) and (7). Equation (6) corresponds to a hyperbola, while Equation (7) is of the type 1:2 with respect to monophenol. Hence, the former predicts that there is no inhibition caused by excess of monophenol (Figure 3), which agrees with the mechanism of Scheme I. Experiments carried out with tyrosinase from other sources (frog skin [18], apple [19] and pear [20]) provided similar results). Equation (7), indicates that inhibition occurs at high monophenol concentrations. To make quantitative studies and to fit a given analytical expression, measurements of the steady-state rate for the enzyme tyrosinase acting on monophenols must be made correctly; this means that the system must have reached its true steady-state and, as mentioned above, this occurs at different times from the beginning of the reaction (Figures 1, 2 and 3)

Action of $6BH_4$

In recent years there has been much discussion concerning the possible regulation of tyrosinase by $6BH_4$. The first work [5] in which such regulation was proposed indicated that $6BH_4$ controls tyrosinase activity by an uncompetitive mechanism requiring the presence of L-tyrosine for effective down-regulation. Furthermore, these authors demonstrated that when L-dopa is the substrate, $6BH_4$ does not inhibit the enzyme, which would imply separate binding sites for L-dopa and L-tyrosine on tyrosinase. In the same work, experimental data showed that tyrosinase was inhibited by an excess of monophenol [5].

In a series of works [4,21], our group proposed the mechanism described in Scheme l, whereby tyrosinase is not inhibited by monophenol [21,22]. However, the inhibition of mushroom tyrosinase by excess of substrate has been described, but note that the absorbance is measured at 475 nm during the first three minutes following the start of the reaction, regardless of the concentration of substrate. This led the above authors to propose a rate equation in the absence of inhibitor as in Equation (7) [5].

It is the form of measuring the enzymatic activity in [5] that is responsible for the error introduced into Equation (7). Therefore when $6BH_4$ or $7BH_4$ were used, the measurements were as those depicted in [5], the authors obtaining an apparent inhibition since the way of measuring was the same. The difference with our model (Scheme I) becomes even more evident when diphenolase activity is measured. According to [5], neither $6BH_4$ nor $7BH_4$ inhibits diphenolase activity, which leads the authors to suggest one active site for L-tyrosine and another for L-dopa. In the case of *o*-diphenols, the method used in [5] is correct since this activity is of the Michaelian type. Based on the above, we conclude that the method used to measure the monophenolase activity of tyrosinase is critical for studying the enzyme's kinetics, both in the presence of substrate alone and in the presence of possible inhibitors (see Figures 1–3).

In a subsequent study, it was demonstrated that $6BH_4$ is oxidised by *o*-quinone [6] and the authors waited sufficient time for the $6BH_4$ to be consumed, observing no inhibition of diphenolase or monophenolase. A similar result was obtained working with ascorbic acid [23]. Although the lag phase was longer, parallel lines were obtained when all the RH_2 was consumed. According to [6], $6BH_4$ inhibits neither of the tyrosinase activities and, therefore, both L-tyrosine and L-dopa must bind to the same active site, which agrees with the mechanism of Scheme I.

In a later work [7], monophenolase activity is again measured at a fixed time after the beginning of the reaction: $\Delta OD_{475nm}/2$ min. Although the authors indicate that this is within the linear region, it again shows inhibition by excess of substrate and, of course, in the presence of $6BH_4$ the apparent inhibition is even greater [7]. As indicated for the case of [7], the cause is the way in which the enzymatic activity is measured, which is critical for enzymes showing a lag period. The possible inhibition of tyrosinase by $6BH_4$ and extrapolation to the possibility of regulating the route from L-phenylalanine to melanin has been discussed in two studies published very close in time [8,9], in which the different explanations for the action of $6BH_4$ and tyrosinase are defended. We shall

focus our attention on an older study, that of Pomerantz, 1966 [11], with which the authors of [8,9] are in agreement. In 1966 Pomerantz demonstrated that 6,7-di-CH_3BH_4 stimulated the tyrosinase hydroxylase activity of mammalian tyrosinase, monitoring the activity by measuring the release of tritium from L-tyrosine-3,5-^{3}H into the solution, in the form of tritiated water (^{3}HOH or TOH) according to [11]. These data are in agreement with the data presented by [6]. Furthermore, Wood et al., [7], agree with Pomerantz in that if the initial concentration of $6BH_4$ ($[6BH_4]_{0)}$ is low (less than 5 μM), $6BH_4$ activates the reaction, while concentrations of $[6BH_4]_0 = 50\,\mu M$, $6BH_4$ inhibit the reaction [5,7–9]. However, Pomerantz, 1966, showed that 6,7-di-CH_3BH_4 at a concentration of 2.4 mM eliminates the lag period, as seen by measuring the formation of TOH, (see Supplementary material, Figure S8). The mechanism proposed in Scheme I can explain these results.

The lag period, τ, is the time taken by tyrosinase, acting on monophenol, to accumulate in the medium a concentration of *o*-diphenol (L-dopa) that we shall call $[D]_{ss}$ The reaction by which *o*-diphenol is generated is described in Scheme 1 as $2Q \rightarrow D + DC$, that is, the stoichiometry will be 2 *o*-quinone/1 *o*-diphenol, and, as a consequence, in the presence of a reductant ($6BH_4$) the concentration of D_{ss} will be reached earlier (stoichiometry 1 *o*-quinone/1 *o*-diphenol). If $[6BH_4]_0 < [D]_{ss}$, the level of D_{ss} is reached earlier and τ diminishes. If $[6BH_4]_0 > [D]_{ss}$, then more *o*-diphenol than necessary is accumulated and the lag period may grow in length (see Supplementary material, Figure S9). However, in the steady-state, the rates will be the same, in the first case during a lag period and in the second during a lag period followed by a burst until the steady-state is reached. Now, if we measure dopachrome at the same time in both cases, the first may show activation and the second an inhibition [5,7–9], but if the formation of TOH is measured, activation is observed and τ decreases [11] (see Supplementary material, Figure S8). Similar results are obtained in the presence of AH_2 [23].

The experiments depicted in Figure 4 confirm what was said previously, namely that, if the absorbance is measured two minutes after the beginning of the reaction, low concentrations of $6BH_4$ (less than $[D]_{ss}$) will produce an apparent activation (curves c and d), compared with what is seen in the absence of $6BH_4$ (curve c). If the concentration of $6BH_4$ is greater than $[D]_{ss}$, the lag period is longer and there is an apparent inhibition, even though measurements made at long times will show parallel lines since the true steady-state will have been reached. In this last case (long times) $V_{ss}^{M,DC}$ are correct and so $V_{ss}^{M,DC}$ vs $[M]_0$ is a hyperbola (Figure 3).

The diphenolase experiments (Figure 5) can be interpreted in the same way: the *o*-quinone generated by the enzyme reacted with the reductant $6BH_4$, in accordance with the chemical reaction depicted in Scheme I ($Q + RH_2 \rightarrow D + Q$); after a lag period, which increased with increasing concentrations of $6BH_4$, the system reached its steady-state with parallel straight lines (traces c–d).

The experiments depicted in Figure 6 also show how the system tries to reach the steady-state. For example, Figure 6 curve (a) and Figure 6 Inset curve (a), show how the system, after the addition of an initial quantity of *o*-diphenol equivalent to $[D]_{ss}$, is in the steady-state at $t = 0$. But when $6BH_4$ is added there is a reaction, $Q + RH_2 \rightarrow D + R$, which involves the accumulation of more *o*-diphenol, which the enzyme eliminates through a burst of activity (see curves b-d of Figure 6 and b–c of Figure 6 Inset). Note how the lines are parallel at long times and how it is once again necessary to measure the rates only after the steady-state has been reached.

This series of experiments supports the following conclusions:

Measuring the diphenolase activity of tyrosinase is not difficult, and the lag period (lasting in the order of milliseconds) will occur in the dead-time. Measuring the monophenolase activity, on the other hand, is more complicated and requires that the system be allowed to reach the steady-state after a lag period. This monophenolase activity is not inhibited by an excess of monophenol. The action of reductants such as $6BH_4$ and 6,7-di-CH_3BH_4 reduces *o*-quinone to *o*-diphenol until all the reductant is used up, at which point the steady-state is reached. Therefore, none of the activities of tyrosinase (diphenolase or monophenolase) is inhibited by these compounds. These results may help explain how reductants act on the melanogenesis pathway.

The experimental behaviour observed is in agreement with the simulation results of Scheme I, which could be observed in the supplementary material (Figures S2– S9).

Acknowledgements

This work was supported in part by grants from the MEC (Spain) Project BIO2006-15363, and from the Fundación Séneca/Consejería de Educación (Murcia), Projects 00672/PI/04, 07 BIO2005/01-6464 and BIO-BMC 06/01-0004. FGM has a fellowship from the MEC (Spain), Reference AP2003-0891. JLM has a fellowship from the MEC (Spain) Reference AP2005-4721.

References

[1] Frieden C. Slow transitions and hysteretic behavior in enzymes. Annu Rev Biochem 1979;48:471–489.

[2] Prota G, Ischia M, Napolitano A. The chemistry of melanins and related metabolites. New York: Oxford University Press; 1998.

[3] Solomon EI, Sundaram UM, Machonkin TE. Multicopper oxidases and oxygenases. Chem Rev 1996;96:2563–2605.
[4] Rodríguez-López JN, Tudela J, Varón R, García-Carmona F, García-Cánovas F. Analysis of a kinetic model for melanin biosynthesis pathway. J Biol Chem 1992;267:3801–3810.
[5] Wood JM, Schallreuter-Wood KU, Lindsey NJ, Callaghan S, Gardner ML. A specific tetrahydrobiopterin binding domain on tyrosinase controls melanogenesis. Biochem Biophys Res Commun 1995;206:480–485.
[6] Jung HJ, Choi SW, Han S. Indirect oxidation of 6-tetrahydrobiopterin by tyrosinase. Biochem Biophys Res Commun 2004;314:937–942.
[7] Wood JM, Chavan B, Hafeez I, Schallreuter KU. Regulation of tyrosinase by tetrahydropteridines and H_2O_2. Biochem Biophys Res Commun 2004;325:1412–1417.
[8] Wojtasek H. Regulation of tyrosinase by tetrahydropterines-what is real? A comment on the work published by Wood et al. on December 24, 2004. Biochem Biophys Res Commun 2005;329:801–803.
[9] Wood JM, Chavan B, Hafeez I, Schallreuter KU. Regulation of tyrosinase by tetrahydropterines – What is real? A critical reanalysis of H. Wojtasek's view. Biochem Biophys Res Commun 2005;331:891–893.
[10] Wood JM, Schallreuter KU. Studies on the reactions between human tyrosinase, superoxide anion, hydrogen peroxide and thiols. Biochim Biophys Acta 1991;1074:378–385.
[11] Pomerantz SH. The tyrosine hydroxylase activity of mammalian tyrosinase. J Biol Chem 1966;241:161–168.
[12] Spencer JD, Chavan B, Marles LK, Kaueser S, Rokos H, Schallreuter KU. A novel mechanism in control of human pigmentation by β-melanocyte-stimulating hormone and 7-tetrahydrobiopterin. J Endocrinol 2005;187:293–302.
[13] Duckworth HW, Coleman JE. Physicochemical and kinetic properties of mushroom tyrosinase. J Biol Chem 1970;245:1613–1625.
[14] Bradford MM. A rapid and sensitive method for the quantization of microgram quantities of protein utilizing the principle of protein-dye binding. Anal Biochem 1976;72:248–254.
[15] Peñalver MJ, Hiner AN, Rodríguez-López JN, García-Cánovas F, Tudela J. Mechanistic implications of variable stoichiometries of oxygen consumption during tyrosinase catalyzed oxidation of monophenols and o-diphenols. Biochim Biophys Acta 2002;1597:140–148.
[16] Gerald CF. Applied Numerical Analysis. Reading: Addison-Wesley; 1978.
[17] García-Sevilla F, Garrido-del Solo C, Duggleby RG, García-Cánovas F, Peyro R, Varón R. Use of a windows program for simulation of the progress curves of reactants and intermediates involved in enzyme-catalyzed reactions. BioSystems 2000;54:151–164.
[18] Ros JR, Rodríguez-López JN, García-Cánovas F. Tyrosinase: Kinetic analysis of the transient phase and the steady-state. Biochim Biophys Acta 1994;1204:33–42.
[19] Espín JC, García-Ruiz PA, Tudela J, Varón R, García-Cánovas F. Monophenolase and diphenolase reaction mechanisms of apple and pear polyphenol oxidases. J Agric Food Chem 1998;46:2968–2975.
[20] Espín JC, Morales M, Varón R, Tudela J, García-Cánovas F. Monophenolase activity of polyphenol oxidase from blanquilla pear. Phytochemistry 1997;44:17–22.
[21] Sánchez-Ferrer A, Rodríguez-López JN, García-Cánovas F, García-Carmona F. Tyrosinase: A comprehensive review of its mechanism. Biochim Biophys Acta 1995;1247:1–11.
[22] Fenoll LG, Peñalver MJ, Rodríguez-López JN, Varón R, García-Cánovas F, Tudela J. Tyrosinase kinetics: Discrimination between two models to explain the oxidation mechanism of monophenol and *o*-diphenol substrates. Int J Biochem Cell Biol 2004;36:235–246.
[23] Ros JR, Rodríguez-López JN, García-Cánovas F. Effect of L-ascorbic acid on the monophenolase activity of tyrosinase. Biochem J 1993;295:309–312.

Supplementary material

The simulation results are in agreement with the experimental data. Simulation was carried out with the computer program WES [1]. The rate constants used for the mechanisms of Schemes SI and SII agree with those used in the bibliography [2]. In the case of the mechanism of Scheme SI, the rate constants used were obtained by our group [3] or fulfil the overall kinetic constant of the steady-state [4].

In the case of a simple mechanism, such as that proposed by Michaelis-Menten (Scheme SI).

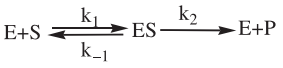

Scheme SI.

The representation of V_{ss}, the steady-state rate of an enzyme acting on a substrate is linear with respect to the enzyme concentration and that of V_{ss} is hyperbolic with respect to substrate concentration (Figure S1), although, even in this simple mechanism, it can be seen that deviations of the typical equilateral hyperbola (inhibition by excess of substrate) can be observed when the complex ES binds another molecule of substrate (Scheme SII) (Figure S1 Inset).

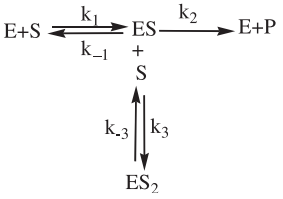

Scheme II.

Note that the dependence V_{ss} *vs* $[E]_0$ is always linear, regardless of whether V_{ss} *vs* $[S]_0$ is hyperbolic or not (Figure S1 Inset).

This simple idea, when transferred to Scheme I proposed for the enzyme tyrosinase acting on monophenols, can be extrapolated when the steady-state rate measurements are made correctly, as shown below.

Figure S1. Dependence of steady-state rates of the mechanism of Scheme SI obtained by simulation, on substrate and enzyme initial concentrations. The rate constants were $k_1 = 10^6\ M^{-1}\ s^{-1}$; $k_{-1} = 10^2\ s^{-1}$; $k_2 = 10^3\ s^{-1}$. Values of V_{ss} obtained by varying the substrate concentration (0.2 mM – 15 mM), with an enzyme concentration of 10 nM. ■ Values of V_{ss} obtained by varying the enzyme concentration (1 nM – 10 nM), with a substrate concentration of 1 mM. Inset. Representation of values of V_{ss} of the mechanism of Scheme SII, obtained by simulation,

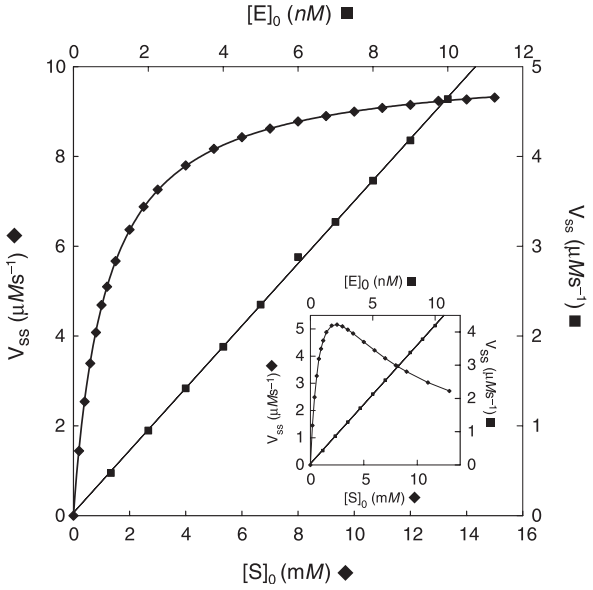

with respect to substrate and enzyme concentrations. Values of V_{ss} obtained by varying the substrate concentration (0.2 mM – 15 mM), with an enzyme concentration of 10 nM. ■ Values of V_{ss} obtained by varying the enzyme concentration (1 nM – 10 nM), with a substrate concentration of 1 mM. The values of k_3 and k_{-3} were $10^5\ M^{-1}\ s^{-1}$ and $5 \times 10^2\ s^{-1}$ respectively.

Figure **S2. Product accumulation, obtained by simulation of Scheme I**. The values of the rate constants were: $k_1 = 1.5 \times 10^5\ M^{-1}s^{-1}$, $k_{-1} = 10.8\,s^{-1}$, $k_2 = 3.8 \times 10^6\ M^{-1}s^{-1}$, $k_{-2} = 10\,s^{-1}$, $k_3 = 3 \times 10^2\,s^{-1}$, $k_4 = 6 \times 10^4\ M^{-1}s^{-1}$, $k_{-4} = 10\,s^{-1}$, $k_{51} = 30\,s^{-1}$, $k_{52} = 24\,s^{-1}$, $k_6 = 4 \times 10^5\ M^{-1}s^{-1}$, $k_{-6} = 10\,s^{-1}$, $k_7 = 200\,s^{-1}$, $k_8 = 2.3 \times 10^7\ M^{-1}s^{-1}$, $k_{-8} = 1.07 \times 10^3\ s^{-1}$, $k_9 = 0.1\,s^{-1}$. Curve (a): the

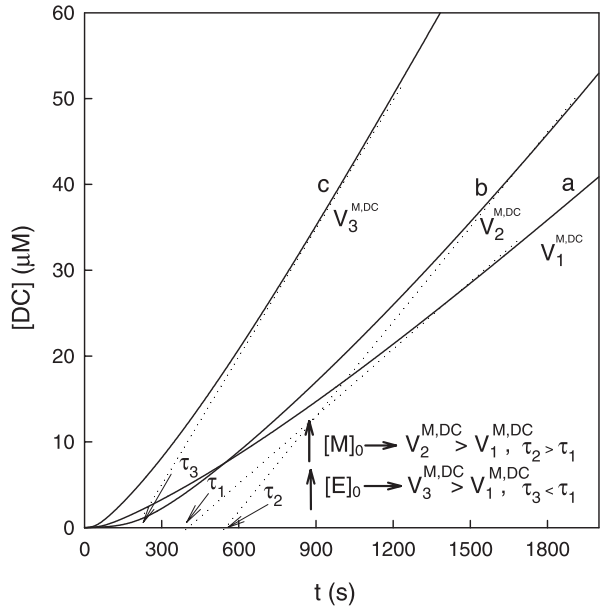

concentrations were: $[M]_0 = 0.2\,mM$; $[E]_0 = 7\,nM$; $[E_m]_0 = 4.9\,nM$; $[E_{ox}]_0 = 2.1\,nM$. Curve (b): $[M]_0 = 1\,mM$, $[E]_0$ same as in (a). Curve (c): $[M]_0 = 0.2\,mM$, $[E]_0 = 14$ nM; $[E_m]_0 = 9.8\,nM$ $[E_{ox}]_0 = 4.2\,nM$; $[O_2]_0 = 0.26\,mM$.

Figure S3. Representation of the values of V_{ss}^{M} and of the lag period corresponding to simulation of the

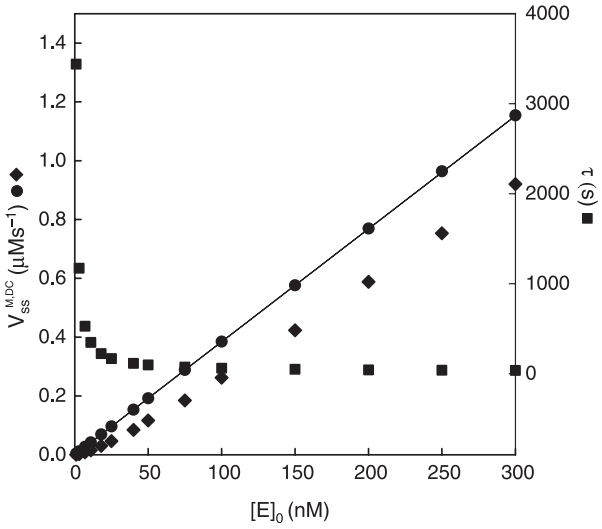

reactions evolving according to the mechanism of Scheme I at different enzyme concentrations. The rate constants of the simulation are the same as in Figure S2. $[M]_0 = 0.2\,mM$. Enzyme concentration varied from 1 nM to 300 nM, with $[E_m]_0 = 0.7 \times [E]_0$ and $[E_{ox}]_0 = 0.3 \times [E]_0$. • Values of V_{ss}^{M} obtained in the true steady-state. ▲ Rate values obtained considering the increase in absorbance at a fixed time from beginning of reaction, three min. ■ Values of lag period.

Figure S4. Representation of the values of V_{ss}^{M} and of the lag period corresponding to simulation of the reactions evolving according to Scheme I with different

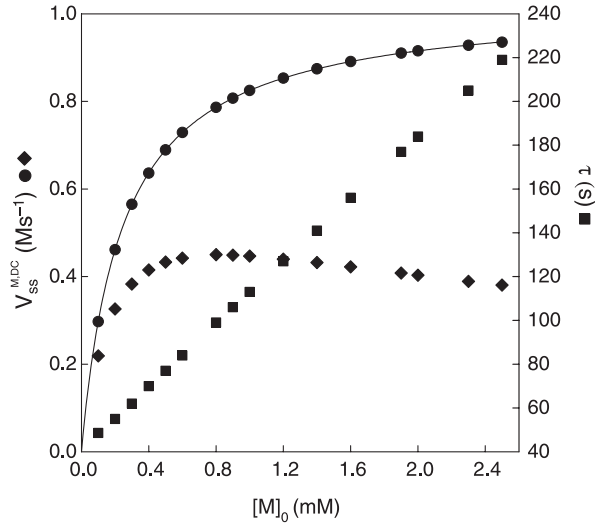

substrate concentrations. The rate constants of the simulation are the same as in Figure S2. The $[M]_0$ varied as indicated in the figure and $[E]_0$ was 120 nM, considering $[E_m]_0 = 0.7 \times [E]_0$ and $[E_{ox}]_0 = 0.3 \times [E]_0$. • Values of V_{ss}^{M} obtained in the true steady-state. ▲ Rate values obtained considering the increase in absorbance at a fixed time from beginning of reaction, three min. ■ Values of lag period.

The simulation of the reactions evolving according to the mechanism of Scheme l, to which the set of differential equations corresponding to the reaction $Q + RH_2 \xrightarrow{k_{12}} D + R$ is added (Scheme I), explains the effect demonstrated by Pomerantz [5] in measuring the formation of TOH from L-tirosine-3,5-^{3}H (Figure S8). When the release of TOH (governed by k_{51}) is simulated in the presence and absence of the reducer of *o*-quinone, activation always occurs in the formation of TOH (Figure S8), as expected and in agreement with [5]. When the reductant is present in the simulation, the $[D]_{ss}$ necessary for the steady-state to be reached, is accumulated earlier and in this way τ decreases, although the same steady-state rate is always reached $V_{ss}^{M,DC}$. Figure S9 shows the accumulation of *o*-diphenol *versus* time in simulations of the reactions evolving according to the mechanism of Scheme I, in the absence of RH_2 and with $[D]_0 = 0$, curve (a) and in the presence of $[D]_0 = D]_{ss}$, curve (b), with $[RH_2]_0 < [D]_{ss}$, curve (c) and with $[RH_2]_0 > [D]_{ss}$, curves (d) – (e) and (f), respectively. Note that, in curve (c), $[D]_{ss}$ is reached before and so the delay in the lag period for accumulating DC is less (apparent activation). However, when $[RH_2]_0 > [D]_{ss}$, the level of [D] exceeds that of $[D]_{ss}$ and the system must reduce it; this it does, but DC accumulates with a longer lag period, curves (d) – (e) and (f) respectively.

Figure S5. Effect of reductants on dopachrome accumulation in the simulation of the reactions evolving according to the mechanism of Scheme I. The rate

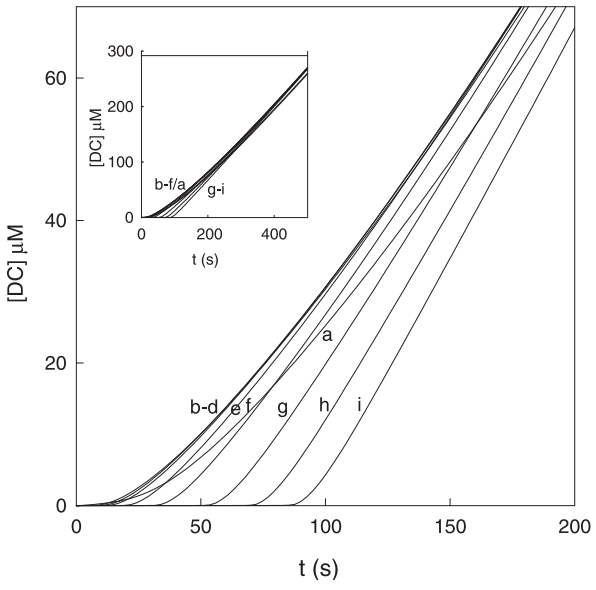

constants are the same as in Figure S2. The initial concentrations of monophenol, E and the reductants (RH_2) were: $[M]_0 = 1$ mM, $[E]_0 = 100$ nM, $[E_m]_0 = 70$ nM, $[E_{ox}]_0 = 30$ nM and RH_2:(a) 0; (b) 2 μM; (c) 3.5 μM; (d) 5 μM; (e) 10 μM; (f) 20 μM; (g) 40 μM; (h) 60 μM; (i) 80 μM, respectively. The Inset represents the same results at longer time, 800 s.

Figure S6. Effect of reductants (RH_2) on product formation (dopachrome), in the simulation of the reactions evolving according to Scheme I with

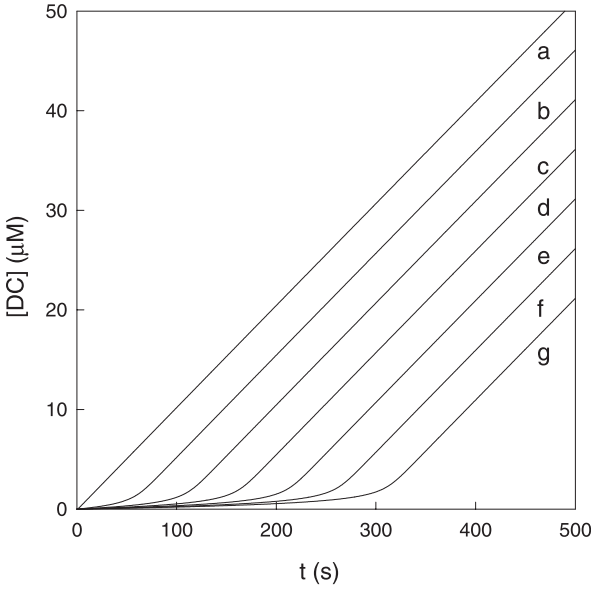

$[M]_0 = 0$. The rate constants are the same as those of Figure S2. $[D]_0 = 1$ mM and $[E]_0 = 3$ nM. The initial concentrations of the RH_2 were: (a) 0; (b) 10 μM; (c) 20 μM; (d) 30 μM; (e) 40 μM; (f) 50 μM and (g) 60 μM, respectively.

Figure S7. Effect of reductants on product formation (dopachrome), in the simulation of the reactions evolving according to the mechanism of Scheme I in the steady-state. The rate constants are the same as in Figure S2. $[M]_0 = 0.9$ mM, $[D]_{ss} = 53.1$ μM, $[E]_0 = 120$ nM. The initial concentrations of RH_2 were: (a) 0; (b) 25 μM; (c) 50 μM and (d) 75 μM.

Figure S8. Effect of reductants on the formation of TOH in the simulation of the reactions evolving according to the mechanism of Scheme I. The rate

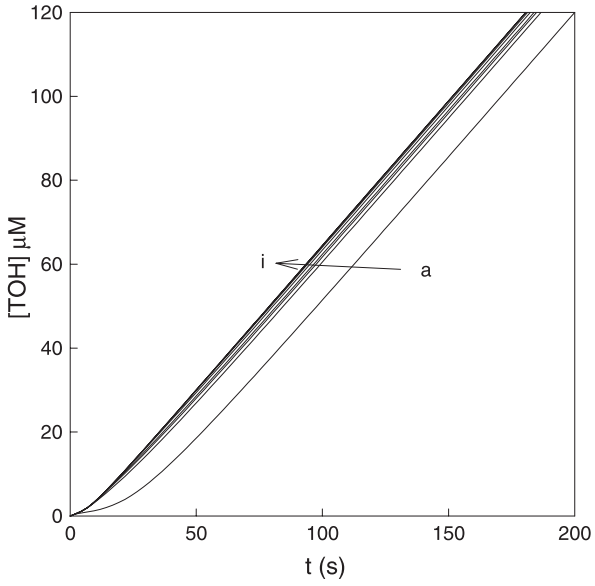

constants are the same as those of Figure S2. $[M]_0 = 0.5$ mM and $[E]_0 = 10$ nM, $[E_m]_0 = 7$ nM, $[E_{ox}]_0 = 3$ nM. The TOH is formed during the step governed by k_{51}, the concentrations of reductant were RH_2: (a) 0; (b)1 μM; (c) 50 μM; (d) 80 μM, respectively.

Figure S9. Effect of reductants on the accumulation of *o*-diphenol in the simulation of the reactions evolving according to the mechanism of Scheme I.

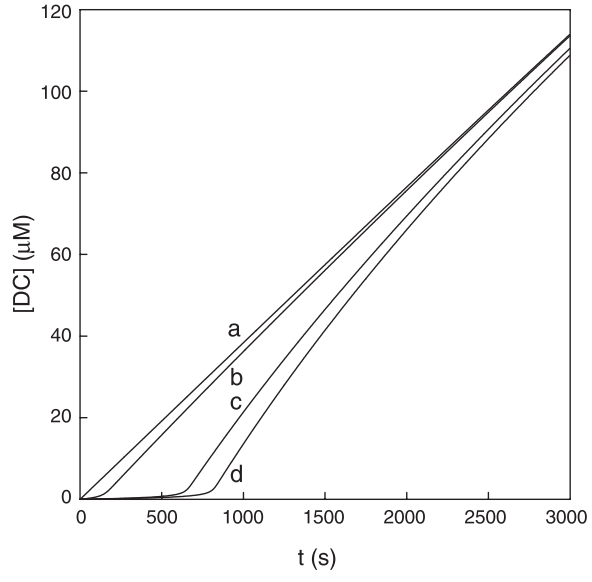

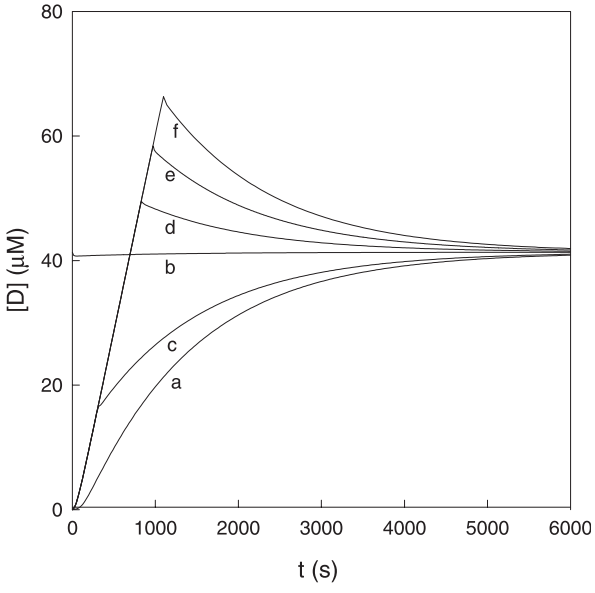

The rate constant are the same as those of Figure S2. $[M]_0 = 0.7\,mM$, and $[E]_0 = 10\,nM$, $[E_m]_0 = 7\,nM$, $[E_{ox}]_0 = 3\,nM$, RH_2 were (a) 0; (b) 0 and $[D] = 41{,}34\,\mu M$; (c) $20\,\mu M$; (d) $80\,\mu M$; (e) $100\,\mu M$ and (f) $120\,\mu M$.

References

[1] García-Sevilla F, Garrido-del Soto C, Duggleby RG, García-Cánovas F, Peyró P, Varón R. Use of a windows program for simulation of the progress curves of reactants and intermediates involved in enzyme-catalyzed reactions. BioSystems 2000;541:51–164.

[2] Hiromi K. Kinetics of fast enzymes reactions. New York, U.S.A.: Halsted Press; 1979.

[3] Rodriguez-Lopez JN, Fenoll LG, García-Ruiz PA, Varón R, Tudela J, Thorneley RN, García-Cánovas F. Stopped-flow and steady-state study of the diphenolase activity of mushroom tyrosinase. Biochemistry 2000;39:10497–10506.

[4] Espín JC, Varon R, Fenoll LG, Gilabert MA, García-Ruiz PA, Tudela J, García Cánovas F. Kinetic characterization of the substrate specificity and mechanism of mushroom tyrosinase. Eur J Biochemistry 2000;267:1270–1279.

[5] Pomerantz SH. The tyrosine hydroxylase activity of mammalian tyrosinase. J Biol Chem 1966;241:161–168.